Microfluid Nanofluid
DOI 10.1007/s10404-007-0177-0

SHORT COMMUNICATION

Electrospinning of hollow and core/sheath nanofibers using a microfluidic manifold

Yasmin Srivastava · Ignacio Loscertales · Manuel Marquez · Todd Thorsen

Received: 13 January 2007 / Accepted: 11 April 2007

Abstract In this article, we describe a microfluidic approach to fabricate hollow and core/sheath nanofibers by electrospinning. Key benefits in using microfluidic devices for nanofiber synthesis include rapid prototyping, ease of fabrication, and the ability to spin multiple fibers in parallel through arrays of individual microchannels. Hollow poly (vinylpyrrolidone) (PVP) + titania (TiO_2) composite and core/sheath polypyrrole (PPy)/PVP nanofibers of the order of 100 and 250 nm, respectively, were successfully fabricated using elastomeric microfluidic devices. Fiber characterization was subsequently carried out using a combination of scanning electron microscopy and transmission electron microscopy.

Keywords Microfluidics · Electrospinning · Composite · Nanofiber · Multiplexed

Y. Srivastava · T. Thorsen (✉)
Department of Mechanical Engineering,
Massachusetts Institute of Technology,
Room 3-246, 77 Massachusetts Avenue,
Cambridge, MA 02139-4307, USA
e-mail: thorsen@mit.edu

Y. Srivastava
Interdisciplinary Network of Emerging Science and Technologies Group Postgraduate Program,
Philip Morris USA, Richmond, VA 23234, USA

I. Loscertales
Escuela Técnica Superior de Ingenieros Industriales,
Universidad de Málaga, Plaza El Ejido s/n,
29013 Málaga, Spain

M. Marquez
NIST Center for Theoretical and Computational Nanosciences,
Gaithersburg, MD 20899, USA

M. Marquez
Harrington Department Bioengineering Arizona State University, Tempe, AZ 85287, USA

M. Marquez
Research Center, Philip Morris USA, 4201 Commerce Road,
Richmond, VA 23234, USA

Polymer nanofibers provide a platform for a number of diverse applications, including drug encapsulation (Jiang et al. 2004; Verreck et al. 2003; Zong et al. 2002), biosensing (Sawicka et al. 2005), filtration (Shin et al. 2005, 2006; Wang et al. 2005) and electronics (Babel et al. 2005; Choi et al. 2003; Liu et al. 2005). Recently, there has been a growing interest in polymer nanofibers with hollow and core/sheath structures, as such structure modifications could further enhance material properties for the aforementioned applications. Many advanced processing techniques, such as template synthesis (Bognitzki et al. 2000; Hou et al. 2002; Steinhart et al. 2002, 2004), self assembly (Wan et al. 2003), and electrospinning (Li et al. 2004, 2005; Loscertales et al. 2004; McCann et al. 2005; Sun et al. 2003; Wei et al.2005), have been employed to make hollow, core/sheath, porous fibers and tubes from natural and synthetic polymers. Kameoka et al.(2003) developed a syringeless, micromachined silicon scanning tip for the electrospinning of oriented nanofibers. Coaxial electrospinning has been extensively exploited as a simple technique to generate hollow and core/sheath nanofibers (Li et al. 2004, 2005; Loscertales et al. 2004; McCann et al. 2005; Song et al. 2005; Sun et al. 2003; Yu et al. 2004; Zhang et al. 2006). Loscertales et al. (2002) used concentric metallic needles to electrospray core/shell monodisperse compound droplets of water coated by olive oil or photopolymer, and later demonstrated a method for making inorganic and hybrid (organic/inorganic) fibers and vesicles

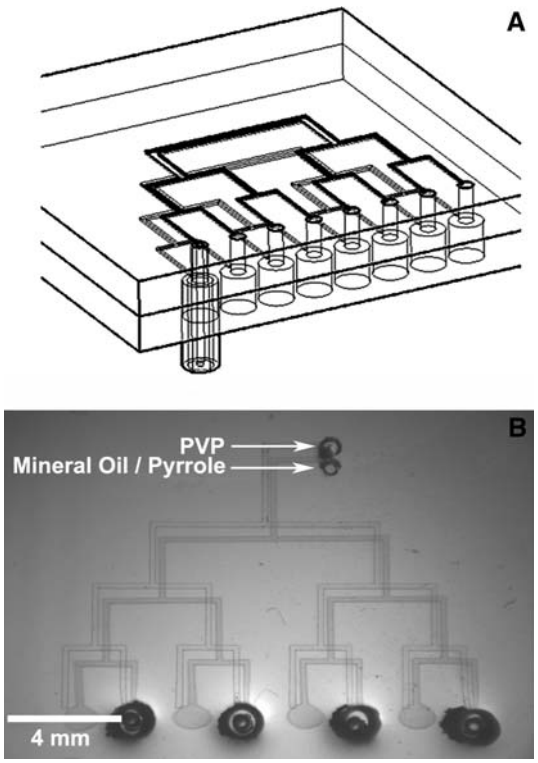

Fig. 1 **a** Schematic representation of the PDMS microfluidic device source using branching microchannel architecture and coaxial spinnerets for parallel electrospinning of hollow and core/sheath type nanofibers. **b** Optical microscopy image of the microfluidic channels illustrating the coaxial spinnerets and connection ports to feed the sheath (PVP) and core (heavy mineral oil or pyrrole + PVP) solutions

via sol-gel chemistry and electrically-forced liquid jets (Larsen et al. 2003; Loscertales et al. 2004). Compound core/sheath nanofibers have also been fabricated by electrospinning using a syringe-in-syringe technique (Sun et al. 2003). Alternatively, concentric spinnerets have also been utilized, using nested capillaries composed of materials like silica (Li and Xia 2004). Li and Xia (2004) used a spinneret consisting of a polymer-coated silica capillary into a stainless steel needle to fabricate ceramic hollow nanofibers. The silica capillary was guided through the wall of a plastic syringe that was hosted on a needle, and connected to another plastic syringe. However, the process of making coaxial-spinnerets is labor-intensive and, to date, has utilized a single spinneret source for generating hollow nanofibers. While mass fabrication of nanofibers has been a subject of research for several years however, reports on multi-jet electrospinning are limited (Ding et al. 2004; Dosunmu et al. 2006; Theron et al. 2005; Tomaszewski et al. 2005), and are mainly restricted to side-by-side electrospinning with multiple syringes, porous tubes or pipes. In this manuscript, we report on a new methodology for the fabrication of hollow and core/sheath nanofibers using a polydimethylsiloxane (PDMS) based microfluidic device that is capable of simultaneously spinning several hollow fibers in parallel. The design (Fig. 1) utilized two layers of microchannels to flow poly (vinylpyrrolidone) (PVP) solution as sheath material and heavy mineral oil or pyrrole + PVP as the core phase through an array of spinners. Two layers of non-intersecting, stacked 100 μm (w) × 100 μm (h) microchannels are arranged in a branching tree pattern to provide constant pressure to each of eight outlet spinnerets. The spinnerets consisted of concentric stainless steel tubes that, when aligned and punched through the elastomer device, focus the core phase in the center of the PVP solution. Advantages of these microfluidic electrospinning devices include ease of fabrication, flexible control over channel dimensions and geometry, and the potential for multiplexed electrospinning within a single microfluidic device (Kameoka et al. 2003; Lin et al. 2005).

The multilayer microfluidic electrospinning devices used in this study were molded from Sylgard 184 PDMS rubber (Dow Corning). Positive-relief photoresist molds, used as masters for the microchannel networks, were fabricated using standard lithographic procedures. To make a master, a 100 μm thick layer of SU8-50 (microchem) was spun on a silicon wafer (1,000 rpm/45 s). After spin-coating, the SU8-50 layer was given a pre-exposure bake of 10 min at 65 °C and 30 min at 95 °C. After baking, the resist was patterned using a UV-mask aligner (Karl Suess) and a negative transparency mask (3,550 dpi, mika color), post-baked for 1 min at 65 °C and 10 min at 95 °C, and developed. After developing, the silicon wafer-based mold was treated with vapor phase trimethylchlorosilane (Aldrich) for 1 min to facilitate mold release.

From the patterned masters, the microfluidic devices were fabricated initially as two independent layers that were later assembled into a composite device using oxygen plasma. For each layer, whose microchannels were used for the sheath and core fluids, respectively, a ~5 mm thick layer of PDMS (5:1 (part A:B)) was poured on the silane-treated mold and baked at 80 °C for 30 min. After the primary cure, the PDMS negative replicas were released from the silicon masters and the fluid inlet and outlet holes were punched with stainless steel luer stubs (McMaster Carr). Different luer stub gauges were used as punches for the inlets (20G) and the respective outlets (15G-sheath layer, 20G-core layer). After punching, the outlets were fitted with stainless steel tubes (New England small tube) (18G-sheath layer, 23G-core layer). For final assembly, the layers were plasma-treated, and subsequently bonded, centering the core outlet tubes within the sheath outlet tubes (Fig. 1b).

Poly (vinylpyrrolidone) was utilized as the base polymer for the electrospinning of hollow and core/sheath nanofibers because of its good solubility in polar solvents and its

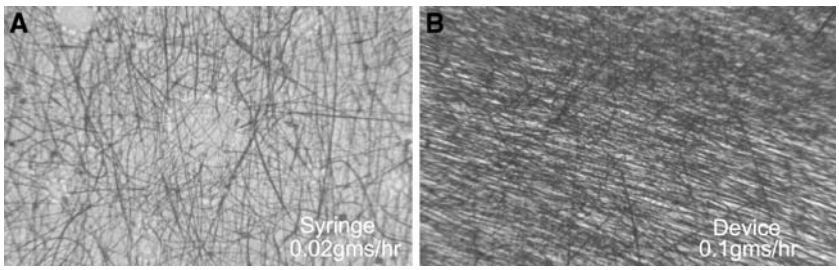

Fig. 2 **a** Optical microscope image of nanofibers fabricated using a syringe based single spinnerette source for electrospinning. **b** Dense network of nanofibrous mat produced using the 8-spinnerette microfluidic PDMS based device

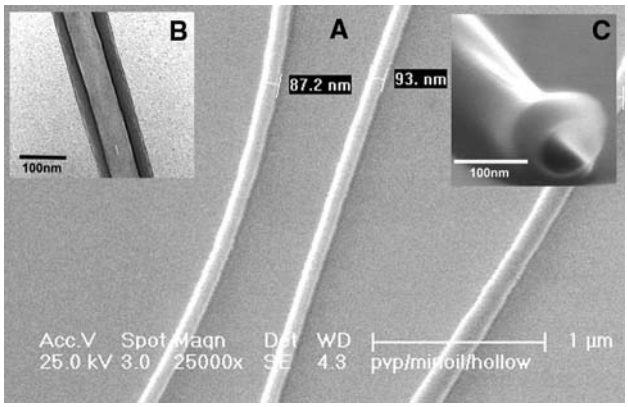

Fig. 3 **a** Scanning electron microscopy (SEM) image of the hollow nanofibers of PVP + TiO_2, indicating the average diameter of hollow nanofibers. **b** Transmission electron microscopy (TEM) image of hollow nanofibers of PVP + TiO_2, revealing the hollow structure after removal of mineral oil core by octane extraction. **c** SEM image of transverse section of PVP + TiO_2 hollow nanofiber

ability to be blended with other functional materials like pyrrole and titanium isopropoxide. For the electrospinning of hollow composite nanofibers in the microfluidic devices, 33% (v/v) of a titanium isopropoxide stock solution (25% (w/v)) $Ti(OiPr)_4$ in ethanol + acetic acid (1:1 v/v)) was added to a 6% (w/v) solution of PVP (mol.wt. 1,300,000, Acros Organics) in ethanol to stabilize the nanofiber sheath by gelation (or cross linking) (Li et al. 2005; Li and Xia 2003, 2004; McCann et al. 2005). The PVP + Ti $(OiPr)_4$ sheath polymer solution was introduced through the microchannels in the bottom sheath layer, while the core material (heavy mineral oil) was fed through the top microchannels. The two flows were controlled independently using syringe pumps (11 Plus, Harvard Apparatus). The typical feeding rate for PVP + Ti $(OiPr)_4$ solution was 0.01 mL/min and for the mineral oil the feeding rate as 0.005 mL/min. To apply a voltage potential to the device for electrospinning, the steel tube connecting the syringe output to the sheath flow device inlet was connected to a high voltage power supply (ES30P-10W, Gamma High Voltage). After the sheath and core flow rates were set, the supply voltage was increased to 15 kV, initiating the formation of bi-component Taylor cones at the spinneret outlets and stable coaxial jets elongated by the applied field.

In the current microfluidic multi-spinneret arrangement, it was observed that mutually interacting electrified jets still undergo bending instabilities characteristic of electrospinning. In addition, it was found that the jets are repulsed from their neighbors due to coulombic forces. Reasonable stability was achieved by increasing the internozzle distance to ~8 mm, yielding more uniform and dense nanofibrous mats. The 8-spinnerette device used in this study produced nanofibers at the rate of 0.1 gh^{-1} compared to spinning from a single needle, which produced nanofibers at the rate of 0.02 gh^{-1} (Fig. 2). Electrospun fibers for SEM/TEM imaging were deposited on carbon coated TEM grids (Ted Pella, Inc.,), and silicon wafer pieces placed on the collector positioned at a distance of 10 cm from the microfluidic source.

Hollow composite nanofibers of PVP + TiO_2 were synthesized from the PVP + TiO_2/heavy mineral oil nanofibers by extracting the mineral oil core with octane. To carry out the extraction, electrospun fibers collected on the silicon wafer and TEM grids were soaked in octane (99 + %, Sigma) for 24 h. The resulting hollow fibers were subsequently imaged by SEM (Philips XL30 FEG) and TEM (JEOL 200CX). A gold layer of 100 Å was sputtered on the surface of the nanofibers to reduce electrostatic charging during SEM imaging. Figure 3 shows SEM and TEM images of hollow PVP + TiO_2 nanofibers fabricated using the coaxial microfluidic electrospinning devices. The hollow nanofibers of PVP + TiO_2 synthesized from the coaxial design are uniform with diameters ranging from 85 to 350 nm with d_{ave} ~ 100 nm. Rapid hydrolysis of Ti $(OiPr)_4$ by the moisture in air leads to the formation of continuous networks (gels) of TiO_2 sols in the PVP sheath layer resulting in robust hollow composite nanofibers.

In addition to the fabrication of hollow nanofibers of PVP, core/sheath PVP nanofibers can be electrospun with the multi-spinneret microfluidic devices by replacing the oil core with functional materials. As an example, we selected polypyrrole (PPy), which possesses high electrical conductivity and good environmental stability (Kanazawa et al. 1979; Kang et al. 2005; Tourillon and Garnier 1982). Conducting core/sheath morphology was achieved by feeding a stock solution of PVP (6% w/v), pyrrole (0.1M)

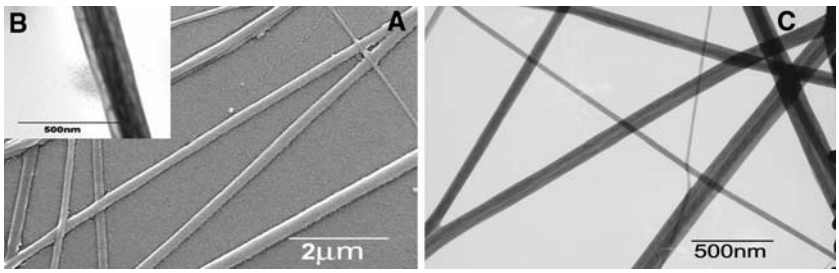

Fig. 4 **a** SEM micrograph of co-electrospun PVP (sheath) and PPy (core) nanofibers indicating the smooth surface morphology. **b** TEM image of PPy/PVP core/sheath single nanofiber showing the uniform encapsulation of PPy in the core, along the fiber axis of PVP. **c** TEM image of PPy/PVP core/sheath multiple nanofibers

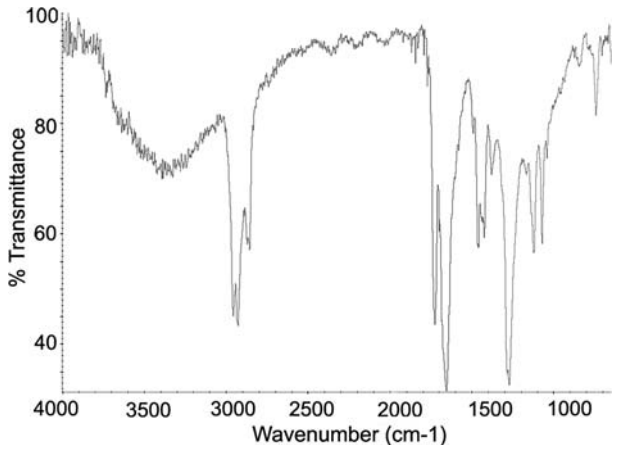

Fig. 5 FTIR-ATR spectra of PPy/PVP core/sheath nanofibers. The IR spectrum reveals PPy peaks at ~3,400, 1,540, 1,470, 1,350, 1,260, 1,070, 1,040, 960, 840, 760 cm^{-1}

and ferric chloride (($FeCl_3$) 2% w/v) in ethanol + DMF (1:1 v/v) through the core channel layer of the microfluidic device and PVP (4% w/v) in ethanol + DMF (1:1 v/v) through the sheath layer. The feed rate for the sheath layer and core layers were 0.01 and 0.005 mL/min, respectively.

The presence of $FeCl_3$ in the core drives the polymerization of pyrrole in the PVP matrix. $FeCl_3$ is an efficient oxidant for pyrrole polymerization, doping chlorine ions in the PPy to make it electrically conducting. Figure 4 shows SEM and TEM images of the PPy/PVP core/sheath nanofibers. A strong contrast between the core and sheath layers is observed in the TEM image, with a PVP sheath wall thickness of ~80 nm. Polypyrrole is encapsulated as a uniform continuous phase in each PVP nanofiber along the axis of the PVP nanofiber. The PPy/PVP core/sheath nanofibers have diameters ranging from 200 to 350 nm with average outer diameters of ~250 nm and average core diameters of the order of ~80 nm. The polymerization of pyrrole in the PVP matrix was confirmed from FTIR spectroscopy (Nicolet Magna 860 FTIR spectrometer) of the composite PPy/PVP nanofibers (Fig. 5) (Kostic et al. 1995).

The broad band at 3,400 cm^{-1} is attributed to N-H stretching vibrations. The peak at 1,540 cm^{-1} is C=C and C–C in ring-stretch mode. The band at 1,470 cm^{-1} is predominantly C=C and C–N stretch modes. The peaks at 1,350 and 1,260 cm^{-1} are C–C in-ring stretch and C–N stretching, the band at ~1,070 cm^{-1} is C–H in-plane bending and ring deformation, and the band at ~1,040 cm^{-1} is C–H ring out-of-plane bending. The form of vibration for the 960 cm^{-1} is complex: C=C stretch, C–C in ring stretch, C–N stretch, C–C inter ring stretch, C=C–C, C–N–C ring deformation, C–H and N–H in plane bending and C–C inter-ring bending. Bands below 800 cm^{-1} originate from the C–H and N–H out-of-plane degrees of freedom. Electrospinning of PPy is traditionally difficult due to its insolubility in most organic solvents. Blending its soluble monomeric precursor, pyrrole, with an appropriate polymer like PVP overcomes these problems, providing a simple method for the electrospinning of composite PPy nanofibers (Li et al. 2006; MacDiarmid et al. 2001; Nair et al. 2005).

Although, repeated exposure of PDMS to organic solvents does effect the channel dimensions, low-solubility solvents can be used with PDMS with minimal swelling and are, therefore, compatible with PDMS microfluidic systems (Lee et al. 2003). In the current investigation, solutions used are based on low-swelling solvents like ethanol and DMF and can be passed through the device channels for fairly long time periods (several hours), while maintaining the reproducibility of nanofiber dimensions and distribution.

In conclusion, we have shown how a coaxial microfluidic device source can successfully be used to electrospin hollow and core/sheath nanofibers. The multi-source microfluidic device enables parallel fiber electrospinning, making the process efficient and versatile for large scale production of nanofibers. Moreover, the simple molding methodology for the elastomeric device fabrication makes it easy to customize the geometry and dimensions of the microchannel networks, enabling the end-user to rapidly fabricate prototype multi-source electrospinning devices.

Acknowledgments This work was partially supported by an INEST grant from Philip Morris USA.

References

Babel A, Li D, Xia YN, Jenekhe SA (2005) Electrospun nanofibers of blends of conjugated polymers: morphology, optical properties, and field-effect transistors. Macromolecules 38(11):4705–4771

Bognitzki M, Hou HQ, Ishaque M, Frese T, Hellwig M, Schwarte C, Schaper A, Wendorff JH, Greiner A (2000) Polymer, metal, and hybrid nano and mesotubes by coating degradable polymer template fibers. Adv Mater 12(9):637–640

Choi SW, Jo SM, Lee WS, Kim YR (2003) An electrospun polyvinylidene fluoride nanofibrous membrane and its battery applications. Adv Mater 15(23):2027–2032

Ding B, Kimura E,Sato T, Fujita S, Shiratori S (2004) Fabrication of blend biodegradable nanofibrous non-woven mats via multi-jet electrospinning. Polymer 45(6):1895–1902

Dosunmu OO, Chase GG, Kataphinan W et al (2006) Electrospinning of polymer nanofibres from multiple jets on a porous tubular surface. Nanotechnology 17(4):1123–1127

Hou HQ, Jun Z, Reuning A, Schaper A, Wendorff JH, Greiner A (2002) Poly (p-xylene) nanotubes by coating and removal of ultrathin polymer template fibers. Macromolecules 35(7):2429–2431

Jiang HL, Fang DF, Hsiao BJ, Chu BJ, Chen WL (2004) Preparation and characterization of ibuprofen-loaded polylactide-co-glycolide/polyethylene glycol-g-chitosan electrospun membranes. J Biomater Sci Polym Ed 15(3):279–296

Kameoka J, Craighead HT et al (2003) Fabrication of oriented polymeric nanofibers on planar surfaces by electrospinning. Appl Phys Lett 83(2):371–373

Kanazawa KK, Diaz AF, Geiss RH, Gill WD, Kwak JF, Logan JA, Rabolt JF, Street GB (1979) Organic metals-polypyrrole, a stable synthetic metallic polymer. J Chem Soc Chem Comm 19:854–855

Kang TS, Lee SW, Joo J, Lee JY (2005) Electrically conducting polypyrrole fibers spun by electrospinning. Synth.Metals 153:61–64

Kostic R, Rakovic D, Stepanyan SA, Davidova IE, Gribov LA (1995) Vibrational spectroscopy of polypyrrole, theoretical-study. J Chem Phys 102(8):3104–3109

Larsen G, Velarde-Ortiz R, Minchow K, Barrero A, Loscertales IG (2003) A method for making inorganic and hybrid (organic/inorganic) fibers and vesicles with diameters in the submicrometer and micrometer range via sol-gel chemistry and electrically forced liquid jets. J Am Chem Soc 125(5):1154–1155

Lee JN, Park C, Whitesides GM (2003) Solvent compatibility of polydimethylsiloxane based microfluidic devices. Anal Chem 75(23):6544–6554

Li D, Xia YN (2003) Fabrication of titania nanofibers by electrospinning. Nano Lett 3(4):555–560

Li D, Xia YN (2004) Direct fabrication of composite and ceramic hollow nanofibers by electrospinning. Nano lett 4(5):933–938

Li D, Babel A, Jenekhe SA, Xia YN (2004) Nanofibers of conjugated polymers prepared by electrospinning with a two-capillary spinneret. Adv Mater 16(22):2062–2066

Li D, McCann JT, Xia YN (2005) Use of electrospinning to directly fabricate hollow nanofibers with functionalized inner and outer surfaces. Small 1(1):83–86

Li XF, Liu CP, Xu D et al (2006) Preparation and properties of sulfonated poly (ether ether ketone)s (SPEEK)/polypyrrole composite membranes for direct methanol fuel cells. J Power Sources 162(1):1–8

Lin T, Wang HX, Wang XG (2005) Self-crimping bicomponent nanofibers electrospun from polyacrylonitrile and elastomeric polyurethane. Adv Mater 17(22):2699–2703

Liu HQ, Reccius CH, Craighead HG (2005) Single electrospun regioregular poly(3-hexylthiophene) nanofiber field-effect transistor. Appl Phys Lett 87(25):253106

Loscertales IG, Barrero A, Guerrero I, Cortijo R, Marquez M, Ganan-Calvo AM (2002) Micro/nano encapsulation via electrified coaxial liquid jets. Science 295(5560):1695–1698

Loscertales IG, Barrero A, Marquez M, Spretz R, Velarde-Ortiz R, Larsen G (2004) Electrically forced coaxial nanojets for one-step hollow nanofiber design. J Am Chem Soc 126(17):5376–5377

McCann JT, Li D, Xia YN (2005) Electrospinning of nanofibers with core-sheath, hollow, or porous structures. J Mater Chem 15(7):735–738

MacDiarmid AG, Jones WE, Norris ID, Gao J, Johnson AT, Pinto NJ, Hone J, Han B, Ko FK, Okuzaki H, Llaguno M (2001) Electrostatically-generated nanofibers of electronic polymers. Synth Metals 119:27–30

Nair S, Natarajan S, Kim SH (2005) Fabrication of electrically conducting polypyrrole-poly (ethylene oxide) composite nanofibers. Macromol Rapid Comm 26(20):1599–1603

Sawicka K, Gouma P, Simon S (2005) Electrospun biocomposite nanofibers for urea biosensing. Sens Actuators B Chem 108(1–2):585–588

Shin C, Chase GG (2006) Separation of water-in-oil emulsions using glass fiber media augmented with polymer nanofibers. J Dispers Sci Technol 27(4):517–522

Shin C, Chase GG, Reneker DH (2005) Recycled expanded polystyrene nanofibers applied in filter media. Colloids Surf A Physicochem Eng Asp 262(1–3):211–215

Song T, Zhang YZ, Zhou TJ, Lim CT, Ramakrishna S, Liu B (2005) Encapsulation of self-assembled FePt magnetic nanoparticles in PCL nanofibers by coaxial electrospinning. Chem Phys Lett 415(4–6):317–322

Steinhart M, Wendorff JH, Greiner A, Wehrspohn RB, Nielsch K, Schilling J, Choi J, Gosele U (2002) Polymer nanotubes by wetting of ordered porous templates. Science 296(5575):1997–1997

Steinhart M, Wehrspohn RB, Gosele U, Wendorff JH (2004) Nanotubes by template wetting: a modular assembly system. Angew Chem Int Ed 43(11):1334–1344

Sun ZC, Zussman E, Yarin AL, Wendroff JH, Greiner A (2003) Compound core-shell polymer nanofibers by co-electrospinning. Adv Mater 15(22):1929–1936

Theron SA, Yarin AL, Zussman E, Kroll E (2005) Multiple jets in electrospinning: experiment and modeling. Polymer 46:2889–2899

Tomaszewski W, Szadkowski M (2005) Investigation of electrospinning with the use of a multi-jet electrospinning head. Fibres Text Eastern Europe 13(4):22–26

Tourillon G, Garnier F (1982) New electrochemically generated organic conducting polymers. J Electroanal Chem 135(1):173–178

Verreck G, Chun I, Rosenblatt J, Peeters J, van Dijck A, Mensch J, Noppe M, Brewster ME (2003) Incorporation of drugs in an amorphous state into electrospun nanofibers composed of a water-insoluble, non-biodegradable polymer. J Control Release 92(3):349–360

Wang XF, Chen XM, Yoon K, Fang DF, Hsiao BS, Chu B (2005) High flux filtration medium based on nanofibrous substrate with hydrophilic nanocomposite coating. Env Sci Tech 39(19):7684–7691

Wan MX, Wei ZX, Zhang ZM, Zhang LJ, Huang K, Yang YS (2003) Studies on nanostructures of conducting polymers via self-assembly method. Synth Metals 135(1–3):175–176

Wei M, Lee J, Kang BW, Mead J (2005) Preparation of core-sheath nanofibers from conducting polymer blends. Macromol Rapid Commun 26(14):1127–1132

Yu JH, Fridrikh SV, Rutledge GC (2004) Production of submicrometer diameter fibers by two-fluid electrospinning. Adv Mater 16(17):1562

Zhang YZ, Wang X, Feng Y, Li J, Lim CT, Ramakrishna S (2006) Coaxial electrospinning of (fluorescein isothiocyanate-conjugated bovine serum albumin)-encapsulated poly (epsilon-caprolactone) nanofibers for sustained release. Biomacromolecules 7(4):1049–1057

Zong XH, Kim K, Fang DF, Ran SF, Hsiao BS, Chu B (2002) Structure and process relationship of electrospun bioabsorbable nanofiber membranes. Polymer 43(16):4403–4412